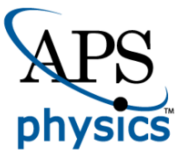

Prediction and Hydrogen Acceleration of Ordering in Iron-Vanadium Alloys

J. Bloch, O. Levy, B. Pejova, J. Jacob, S. Curtarolo, and B. Hjörvarsson

Phys. Rev. Lett. **108**, 215503 — Published 25 May 2012

DOI: 10.1103/PhysRevLett.108.215503

Prediction and hydrogen-acceleration of ordering in iron-vanadium alloys

J. Bloch,[1,2] O. Levy,[2] B. Pejova,[1,3] J. Jacob,[1] S. Curtarolo,[4] and B. Hjörvarsson[1]

[1] *Department of Physics, University of Uppsala, Box 530, SE-75121, Uppsala, Sweden*
[2] *Department of Physics, NRCN, P.O.Box 9001, Beer-Sheva, Israel*
[3] *Institute of Chemistry, Faculty of Science, Sts. Cyril and Methodius University, Skopje, Macedonia*
[4] *Department of Mechanical Engineering and Materials Science and Department of Physics, Duke University, Durham, NC 27708*

Ab initio calculations of binary metallic systems often predict ordered compounds in contrast to empirical reports of solid solutions or disordered phases. These discrepancies are usually attributed to slow kinetics that retains meta-stable structures at low temperatures. The Fe-V system is an example of this phenomenon, in which we predict two ordered stable groundstates, Fe_3V and FeV_3, whereas a disordered σ-phase is reported. We propose to overcome this difficulty by hydrogen absorption, which facilitates metal atom mobility through vacancy formation and separation between the two elements due to their opposite affinities towards it, thus accelerating transformation kinetics. Hydrogen also increases the relative stability of the ordered structures compared with that of the σ-phase without affecting the shape of the phase diagram. The hydrogen-induced formation of the ordered structures is expressed by a reversible decrease of the electrical resistivity with increasing hydrogen pressure. Such behavior has not been reported before in thin H absorbing films. Formation of the ordered structures is further substantiated by the kinetics of the resistivity changes upon variation of the hydrogen pressure, where two stages are distinguished: a fast initial stage and a much slower subsequent process in which the resistivity changes direction, associated with hydrogen dissolution and phase transformation, respectively.

The development of efficient calculation methods based on density functional theory (DFT) together with the fast progress of computer technology have transformed the ability of materials scientists to describe the properties of complex materials and apply it to the design and discovery of new materials [1–10]. In particular, ground-state predictions of binary crystal structures using high-throughput *ab initio* methods have been found to be highly accurate, with reliability of up to 97% [10]. The comparison between predicted structures and empirical phase diagrams may be difficult due to entropy and kinetic effects. Real systems are usually measured above room temperature, where entropy may direct the system towards states less ordered than its ground state when the formation-energies of several structures are close enough. One expects that cooling down the system will recover the ground-state structure. However, transformation kinetics slows exponentially with decreasing temperatures, which may confine the system to a metastable state, preventing altogether the emergence of the groundstate.

In this letter we present predictions of a high-throughput *ab initio* calculation of unobserved stable groundstates in the FeV binary system and apply an experimental method that mitigates the above difficulties to assess them. The FeV system has attracted considerable attention due the presence of a stable disordered σ phase and a metastable A2-B2 disorder-order phase transition at elevated temperatures [11]. This ordering has been recently shown to be accompanied by phonon-softening, a behavior that has not been reported previously for any system in which there is no change in symmetry of the underlying parent lattice [12]. FeV multilayers have been studied as hydrogen absorption devices due to the large exothermic solubility of hydrogen in vanadium and its fast diffusion and low solubility in iron [13].

The Fe-V phase diagram consists of a continuous solid solution at elevated temperatures and an extensive σ phase that forms congruently from it near equiatomic stoichiometry [14]. The σ phase is a disordered phase of prototype $Cr_{0.49}Fe_{0.51}$ (space group $P4_2/mnm$) with 30 atoms per unit cell distributed among five nonequivalent Wyckoff positions. The phase diagram suggests that the low temperature boundaries of the homogeneous σ phase converge into a stoichiometric composition FeV_2. It should be noted, however, that no experimental data is available for this system below 600°C and the trends shown in the diagram below this temperature are extrapolations based on thermodynamic data [14].

Ab initio calculations of the energies of 250 crystal structures spanning the entire concentration range of the FeV system were performed using the high-throughput framework AFLOW [15] employing the Vienna Ab initio Simulation Package-VASP [16]. Details of the calculation method appear in [9, 10]. The detailed results for all the calculated structures are available on the Materials Genome Repository, www.aflowlib.org. The zero temperature phase diagram, the convex hull of the system, is made of the extremal low-energy structures at the various concentrations. It is predicted to include, in addition to the pure elements bcc structures, two stable compounds Fe_3V ($D0_3$) and FeV_3 (A15). It is shown in Fig. 1, together with the 32 ordered realizations of the σ phase and the metastable B2 phase. According to the empiri-

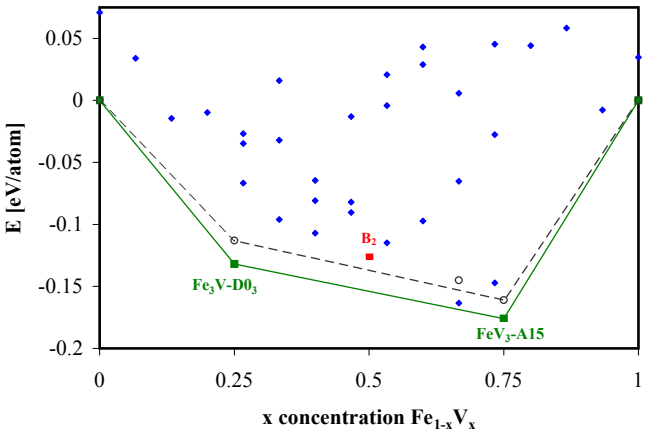

FIG. 1: (color online) The FeV convex hull showing two stable compounds (green squares), the 32 ordered realizations of the σ-phase (blue diamonds) and the metastable B2 phase. The circles show the formation energies of the compounds and the lowest energy σ configuration in the presence of 3at% hydrogen loading. The dashed line is the corresponding convex hull.

cal phase diagram $Fe_{10}V_{20}$ is the only stable composition of the σ phase at low temperatures [14]. This is in agreement with the DFT results, that show this realization as the lowest energy σ state, just 5 meV/atom above the FeV_3-Fe_3V tie-line. The B2 phase is 29 meV/atom above this tie-line.

The difficulties encountered in experimentally studying FeV alloys below 600°C, due to slow kinetics, may render the observation of the predicted structures improbable. However, the kinetics can be accelerated using a catalyzing agent, e.g. hydrogen. It is known that dissolved hydrogen can enhance metal atom diffusion and induce phase separation, e.g. in a variety of Pd-rich alloys [17]. Even relatively small amounts of dissolved hydrogen allow phase separation to take place faster and at lower temperatures than in its absence [18]. At low concentrations, hydrogen generally dissolves interstitially in transition metals without changing their crystal structure. The solubility of hydrogen in vanadium is relatively large and exothermic, whereas in iron it is very small and endothermic. The heat of solution of hydrogen in vanadium and iron is 0.3eV and -0.28eV, respectively [19]. The difference in the affinities toward hydrogen of iron (repulsive) and vanadium (attractive) may further promote phase separation since vanadium atoms tend to accumulate in the vicinity of the H atoms whereas iron atoms are repelled from them. In Pd_3Mn, for example, it has been found that octahedral interstices for which only Pd atoms are nearest neighbors are preferentially occupied by deuterium atoms whereas those having also Mn as nearest atoms are much less occupied [20].

To study the effect of dissolved hydrogen we calculated the energies of the stable structures with a hydrogen atom occupying interstitial sites. We find that the octahedral site is the most favorable for hydrogen in bcc iron whereas the tetrahedral site is the most favorable in bcc vanadium. In the ordered structures of Fe_3V and FeV_3, we used AFLOW, implementing a combinatorial method described in Ref. [21], to identify 5 and 6 symmetrically inequivalent interstitial sites, respectively. The most favorable of these are shown in Fig. 2. In the σ phase, AFLOW finds 17 possible interstitial sites, the most favorable of which is also shown in Fig. 2. Calculating the appropriate averages of the energies in unit cells with and without interstitials, we find that while the energies of the structures in Fig. 2 are higher in the presence of a given small concentration of dissolved hydrogen, as expected, the shape of the phase diagram is not affected (see Fig. 1). The ordered Fe_3V and FeV_3 compounds are still the most stable and the $Fe_{10}V_{20}$ phase is metastable, with energy above the $D0_3$-A15 tie-line that is higher in the presence of hydrogen, 8meV/atom compared to 5meV/atom before loading. This indicates that the predicted ordered structures are relatively more stable and are more likely to form following hydrogen absorption.

The qualitative difference in the disorder-order transition between the σ and the ordered phases should be easily followed by changes in the electrical conductivity [22]. Such measurements have been widely applied for research of hydrogen interaction and hydrogen induced order-disorder transitions in metals [23], especially in thin films [24]. We measured 10nm films of $Fe_{1-x}V_x$ (x=0.5,0.9,1) grown on a $10\times10\times0.5$ mm^3 polished single crystal MgO(001) substrate using UHV-based magnetron cosputtering. The samples were deposited from targets of iron and vanadium onto the substrate held at 573K, and capped with 5 nm of palladium after cooling to room temperature, to facilitate hydrogen loading and protect against oxidation. The film resistivities at 423K were 10.5Ω (x=0.5), 17.5Ω (x=0.9) and 12.4Ω (x=1). A detailed description of the experimental setup is given in reference [25]. Fig. 3 shows results for vanadium and $Fe_{0.5}V_{0.5}$ films. A V(001) film at 423K is used as a reference, demonstrating the characteristic increase of the resistivity with increased concentration of dissolved hydrogen. The resistivity of a metal containing interstitial hydrogen atoms includes a temperature-independent contribution from electron-hydrogen scattering. For low H concentrations the relation between this excess resistivity, R, and the concentration c_H (expressed as [H/V]) is given by the modified Nordheim equation [23]:

$$R = Kc_H\,(n - c_H)\,, \qquad (1)$$

where n is a limiting concentration which depends on the geometry of the metal lattice and the type of site

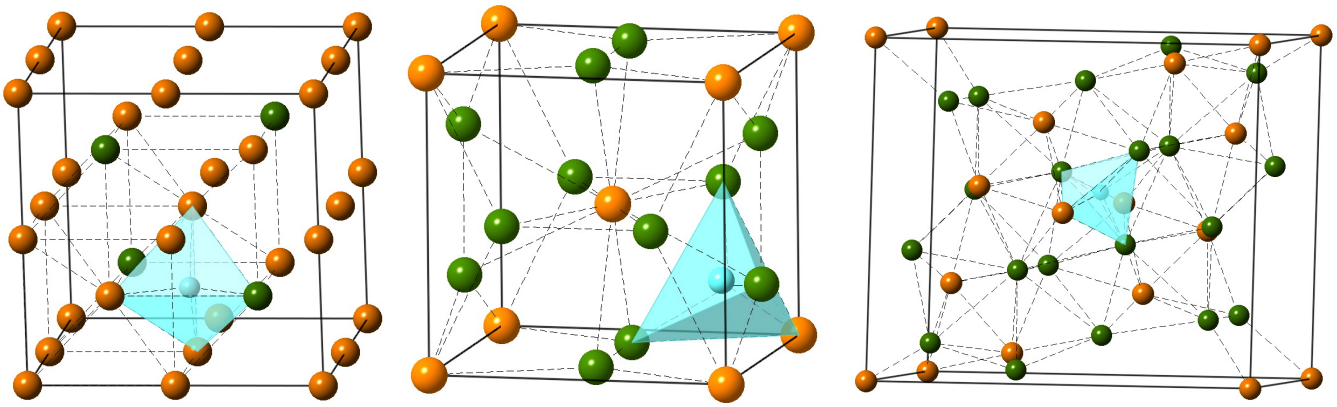

FIG. 2: (color online) The conventional unit cells of Fe_3V-$D0_3$ (left), FeV_3-A15 (center) and $Fe_{10}V_{20}$-σ phase (right), with occupied most favorable interstitial sites (light blue tetrahedrons). Iron atoms in orange, vanadium in green and hydrogen in blue.

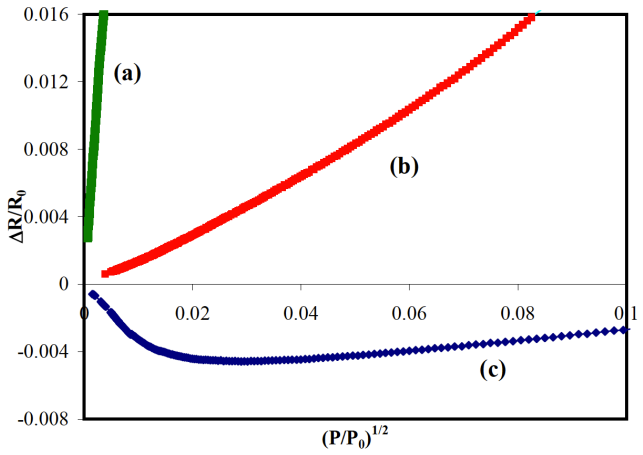

FIG. 3: (color online) Relative residual resistivity vs. hydrogen pressure isotherms of 10nm films of (a) Vanadium at 423K; (b) $Fe_{0.5}V_{0.5}$ alloy at 310K; (c) $Fe_{0.5}V_{0.5}$ alloy at 423K.

occupied, and K is a constant. R is thus proportional to c_H when $c_H \ll n$. Curve (a) in Fig. 3 represents this relation between hydrogen concentration and pressure. At sufficiently low hydrogen concentrations, its solubility in the metal obeys Sievert's law [26]:

$$\left(\frac{P_{H2}}{P_0}\right)^{\frac{1}{2}} = K_s\,(T)\,c_H, \qquad (2)$$

where P_0 is a reference pressure, usually taken as 1bar. $K_s(T)$ is the dimensionless temperature-dependent Sievert's constant. Thus, by combining Eqs. (1) and (2), R is expected to increase linearly with $P_{H_2}{}^{\frac{1}{2}}$, as is actually observed for the pure vanadium film. At relatively low temperatures, the residual resistivity of a $Fe_{0.5}V_{0.5}$ film, curve (b) in Fig. 3, increases with hydrogen pressure, but with a significant deviation from linearity. Comparison of curves (a) and (b) indicates that the H solubility in the $Fe_{0.5}V_{0.5}$ alloy is much lower than in pure vanadium, as expected [27]. The difference in hydrogen concentration at the same P_{H_2} is more than an order of magnitude. The difference at the same temperature should be even higher, since for pure vanadium the solubility of H increases as temperature decreases [25].

At a higher temperature, Fig. 3(c), the residual resistivity unexpectedly decreases with increasing hydrogen pressure right from the initial addition of hydrogen to the system, reaching a minimum at $P_{min} \approx 90$Pa. Decrease of the residual resistivity in thin metallic films has been previously observed only following an initial increase to a maximum, and associated with formation of ordered structures [28]. Initial decrease of R was seen in the bulk in only one alloy system, AgPd [29, 30]. We observed a similar, but much smaller, negative residual resistivity in a $Fe_{0.1}V_{0.9}$ thin film at 523K with $P_{min} \approx 7$Pa. Above 10Pa, the resistivity returns to the normal behavior, increasing with hydrogen pressure. At lower temperatures, the change in R under pressures below 10Pa was unstable. Below 370K this effect is no longer observed and R increases linearly with $P^{\frac{1}{2}}$.

The decrease of the residual resistivity of $Fe_{1-x}V_x$ can be explained, as mentioned above, by hydrogen acting as a catalyzing agent for the formation of at least one of the predicted ordered structures. An alternative explanation might be related to hydrogen-induced changes in the electronic band structure and density of states, without phase transformation, that affect the scattering of the conduction electrons. Such a phenomenological explanation was proposed for the decrease of the resistivity with increasing hydrogen content observed in $Ag_{1-x}Pd_x$ wires ($0.5 < x < 0.7$) at room temperature [29] and 4.2K [30]. This does not seem the case for FeV. The concentration of H in the $Fe_{0.5}V_{0.5}$ alloy is much smaller than in the AgPd alloys, whereas the resistivity change is comparable. In addition, electronic structure calculations for the $Fe_{10}V_{20}$ σ-phase, without and with interstitial hydrogen (Fig. 4), indicate negligible hybridization of hydrogen s-states with the dominant d-band character of

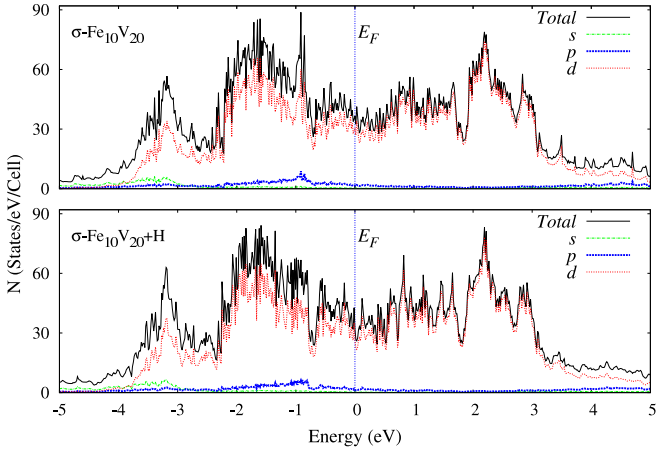

FIG. 4: (color online) The electronic densities of states of $Fe_{10}V_{20}$ σ-phase without and with interstitial hydrogen in the favorable site shown in Fig. 2(c).

the Fe-V bonding. This implies that hydrogen introduction does not lead to any appreciable modification of the electronic structure. More importantly, the differences in the density of states in the vicinity of the Fermi energy are negligible. Therefore it seems very unlikely that the mechanism of enhanced electron scattering could be sufficient to produce the resistivity changes actually observed in Fig. 3(c). It should be noticed that the possible existence of ordered groundstates in the Ag-Pd system has not been considered as an explanation in [30], since the available empirical data shows complete miscibility of the fcc phase for all concentrations. However, recent *ab initio* calculations indicate that such ordered ground states should exist in this system, similarly to the FeV system studied here [10].

In addition, changes in the electronic structure cannot account for the kinetic behavior during absorption or desorption of hydrogen. In Fig. 5 the kinetics of hydrogen desorption at 423K is compared for pure vanadium and $Fe_{0.1}V_{0.9}$ alloy 10nm films (a similar effect is observed in the $Fe_{0.5}V_{0.5}$ film). The upper graph describes the change in resistivity of the vanadium film, with a simultaneous decrease in hydrogen pressure during a desorption step. The resistivity decreases with the pressure because the number of scattering centers is decreased as H atoms desorb from the film. It is obvious that the resistivity follows closely the changes in pressure, as expected. A quite different behavior is observed for the $Fe_{0.1}V_{0.9}$ alloy shown in the lower figure. The initial behavior follows almost exactly that of the vanadium sample, namely the resistivity decreases with pressure. However, when the pressure is stabilized, a second stage starts, in the opposite direction. This stage is slow compared with the initial stage. Similar, but opposite behavior is observed for hydrogen absorption at low pressures, below approximately 20Pa.

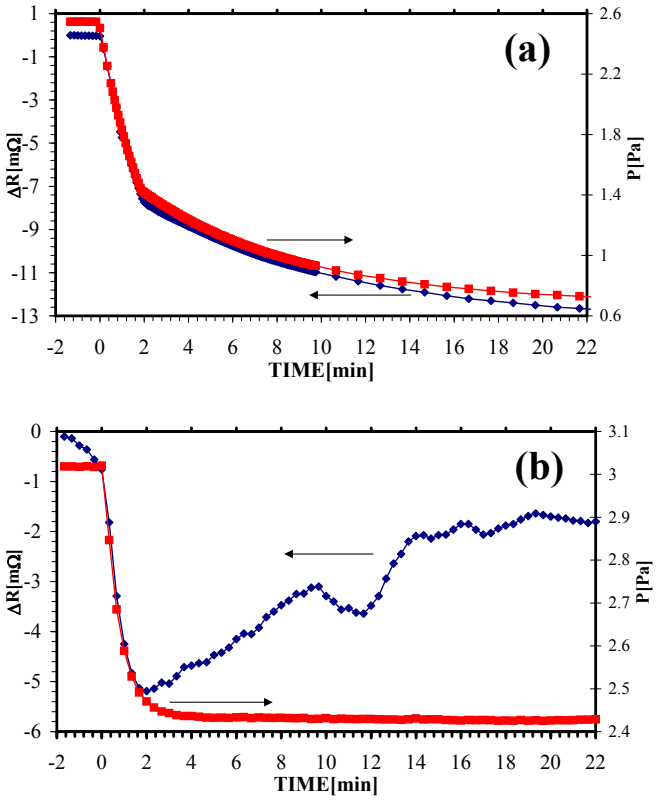

FIG. 5: (color online) Resistivity changes (diamonds) with hydrogen pressure (squares) at 423K for 10nm films of (a) vanadium and (b) $Fe_{0.1}V_{0.9}$ alloy [31].

Hydrogen induced phase separation can account for this peculiar kinetic behavior. The process of phase formation associated with metal atoms diffusion is slow compared to hydrogen dissolution in the film. Thus it is expected that two stages will be observed as the sample is exposed to hydrogen. Initially, the hydrogen dissolved in the film will increase the resistivity normally by serving as scattering centers in the metal lattice. Then, a slower process of phase separation will take place in which the resistivity is changed in the opposite (decrease) direction. For desorption the process is reversed as shown in Fig. 5(b); during the first stage, H atoms dissolved in the metal lattices of the predicted ordered phases desorb from the film. The number of the associated scattering centers is reduced, leading to a decrease of the resistivity with the pressure, similar to the behavior of the reference pure vanadium film (Fig. 5(a)). Near the minimum in resistivity the phase separation is reversed, due to the higher entropy of the disordered σ-phase and the smaller formation-enthalpy differences in the absence of absorbed hydrogen, leading to an increase in the residual resistivity. Additional discussion of this measurement is provided in the supplementary material [31].

In conclusion, this work presents evidence that using hydrogen as a catalyzing agent could help overcome the

kinetic restrictions preventing the transformation of a binary alloy system from its high temperature structure to ground state crystal structures. This method is applied to the FeV system in which calculated ground state structures differ from the high temperature experimentally observed one. This method may be applied to other systems and bridge some of the current discrepancies between available experimental data and predictions of *ab initio* calculations [9].

The authors acknowledge Kesong Yang and Shidong Wang for fruitful discussions. SC acknowledges partial support of ONR (N00014-11-1-0136, N00014-09-1-0921), and NSF (DMR-0639822).

[1] G. H. Jóhannesson, T. Bligaard, A. V. Ruban, H. L. Skriver, K. W. Jacobsen, and J. K. Nørskov, Phys. Rev. Lett. **88**, 255506 (2002).
[2] S. Curtarolo, D. Morgan, K. Persson, J. Rodgers, and G. Ceder, Phys. Rev. Lett. **91**, 135503 (2003).
[3] D. P. Stucke and V. H. Crespi, Nano Lett. **3**, 1183 (2003).
[4] J. Greeley and M. Mavrikakis, Nat. Mater. **3**, 810 (2004).
[5] A. R. Oganov and C. W. Glass, J. Chem. Phys. **124**, 244704 (2006).
[6] V. Ozolins, E. H. Majzoub, and C. Wolverton, Phys. Rev. Lett. **100**, 135501 (2008).
[7] C. Ortiz, O. Eriksson, and M. Klintenberg, Comp. Mat. Sci. **44**, 1042 (2009).
[8] J. Hafner, J. Phys.: Conden. Matt. **22**, 384205 (2010).
[9] O. Levy, R. V. Chepulskii, G. L. W. Hart, and S. Curtarolo, J. Am. Chem. Soc. **132**, 833 (2010).
[10] S. Curtarolo, D. Morgan, and G. Ceder, Calphad **29**, 163 (2005).
[11] J.-I. Seki, M. Hagiwara, and T. Suzuki, J. Mater. Sci. **14**, 2404 (1979).
[12] J. A. Muñoz, M. S. Lucas, O. Delaire, M. L. Winterrose, L. Mauger, C. W. Li, A. O. Sheets, M. B. Stone, D. L. Abernathy, Y. Xiao, et al., Phys. Rev. Lett. **107**, 115501 (2011).
[13] F. Stillesjö, B. Hjörvarsson, and B. Rodmacq, J. Magn. Magn. Mat. **126**, 102 (1993).
[14] J. F. Smith, Bull. Alloy Phase Diagrams **5**, 184 (1984).
[15] S. Curtarolo, W. Setyawan, G. L. W. Hart, M. Jahnatek, R. V. Chepulskii, R. H. Taylor, S. Wang, J. Xue, K. Yang, O. Levy, M. Mehl, H. T. Stokes, D. O. Demchenko, and D. Morgan, Comp. Mat. Sci. **58**, 218-226 (2012).
[16] G. Kresse and J. Hafner, Phys. Rev. B **47**, 558 (1993).
[17] T. B. Flanagan and C. N. Park, J. Alloys Comp. **293-295**, 161 (1999).
[18] H. Noh, J. D. Clewly, T. B. Flanagan, and A. P. Craft, J. Alloys Comp. **240**, 235 (1996).
[19] H. Wipf, *Hydrogen in Metals III* (Springer, Berlin, 1997), vol. 73, p. 1.
[20] P. J. Ahlzn, Y. Andersson, R. Tellgren, D. Rodic, T. B. Flanagan, and Y. Sakamoto, Z. Phys. Chem. N.F. **163**, 213 (1989).
[21] R. V. Chepulskii and S. Curtarolo, Phys. Rev. B **79**, 134203 (2009).
[22] S. Flügge, *Encyclopedia of Physics, Vol. XIX, Electrical conductivity* (Springer-Verlag, Berlin, 1956).
[23] J. A. Pryde and I. S. T. Tsong, Acta Metal. **19**, 1333 (1971).
[24] H. Zabel and B. Hjörvarsson, *Progress in Hydrogen Treatment of Materials* (Donetsk, 2001).
[25] J. Bloch, B. Pejova, J. Jacob, and B. Hjörvarsson, Phys. Rev. B **82**, 245428 (2010).
[26] Y. Fukai, *The Metal-Hydrogen System, Basic Bulk Properties, Springer Series in Materials Science, Vol. 21* (Springer-Verlag, Berlin, 1993).
[27] P. Perrot, *Iron-Hydrogen-Vanadium, in Group IV Physical Chemistry Numerical Data and Functional Relationships in Science and Technology* (Springer, Berlin, 2008), vol. 11.
[28] J. Bloch, B. Hjörvarsson, S. Olsson, and R. Brukas, Phys. Rev. B **75**, 165418 (2007).
[29] A. W. Carson, F. A. Lewis, and W. H. Schurter, Trans. Faraday Soc. **63**, 1447 (1967).
[30] G. Bambakidis, R. J. Smith, and S. A. Otterson, Phys. Stat. Solidi (A) **26**, 53 (1974).
[31] See EPAPS Document No. XXXX for supplementary material. For more information on EPAPS, see http://www.aip.org/pubservs/epaps.html.